*An improved Antarctic dataset for high resolution numerical ice sheet models (ALBMAP v1)* *February 2010*

Authors: Anne M. Le Brocq[1,2], Antony J. Payne[3] and Andreas Vieli[1]. Contact a.lebrocq@exeter.ac.uk.

Other contributors: Robert Athern[4], Jonathan Bamber[3], Josefino Comiso[5], Laura Edwards[6], Cathrine Fox Maule[7], Jennifer Griggs[3], Frank Nitsche[8], Nicholai Shapiro[9], Michiel Van den Broeke[10] and David Vaughan[4] & AGASEA/BBAS (see end of document for affiliations).

## *1. Introduction*

The dataset described in this document has been put together for the purposes of numerical ice sheet modelling of the Antarctic Ice Sheet (AIS), containing data on the ice sheet configuration (e.g. ice surface and ice thickness) and boundary conditions, such as the surface air temperature and accumulation. It is now possible to download a community ice sheet model (e.g. Glimmer-CISM, Rutt et al., 2009), but without adequate data it is difficult to utilise such models. More specifically, ice sheet models that are initialised and run forward from the present day ice sheet configuration, need input data to represent the present-day ice sheet configuration as closely as possible (unlike those spun-up from ice free conditions, which only require the bed/bathymetry). Whilst the BEDMAP dataset (Lythe et al., 2001) was a step forward when it was made, there are a number of inconsistencies within the dataset (see Section 3), and since its release, more data has become available. The dataset described here incorporates some major new datasets (e.g. AGASEA/BBAS ice thickness, Nitsche et al. (2006) bathymetry), but by no means incorporates all the new data available. This considerable task is left for a 'BEDMAP2', (an updated version of BEDMAP), however, the processing carried out in this document illustrates the requirements of a dataset for the purpose of high resolution ice sheet modelling, and bridges the gap until a BEDMAP2 is published. It is envisaged, however, that updated versions of the data set will be made available periodically when new regional data sets become available and can be readily incorporated.

Whilst the ice sheet configuration datasets described here may be used for purposes other than ice sheet modelling, the user should be aware that the focus of the data preparation was on assembling a dataset suitable for ice sheet modelling. For example, no claims are made about the accuracy of the sub-ice shelf interpolation, only that it is a 'best guess' which ensures the ice shelf floats and has a reasonable cavity underneath it. This document does not attempt to consider or quantify dataset errors, the reader is referred to original references for this.

This document describes the data processing carried out to produce the final datasets (it is intended to submit a publication to Earth System Science Data in the near future). Firstly, the ice sheet configuration datasets are described (Sections 2 & 3), then the surface temperature (Section 4), the accumulation (Section 5) and finally the geothermal heat flux (Section 6).

### *1.1 Dataset overview & format*

Table 1 lists the data available in the overall dataset and provides an indication of the various sources of data. For a full description see the relevant section in this document.

The data are provided in a netcdf data format, see http://www.unidata.ucar.edu/software/netcdf/ for more details of this data format. Tools to convert the data are available, for example, in Matlab and ArcGIS (9.2 onwards).

The data are on a 5 km resolution grid, in a Polar Stereographic Projection (Central Meridian, 0°, Standard Parallel, - 71°S) with respect to to EIGEN-GLO4C geoid. The 5 km grid is 1160 columns by 1120 rows, the lower left corner (corner of the lower left cell) is -2800000 m, -2800000 m. The nodata value is -9999. Densities used are 1028 kg $m^{-3}$ for ocean water and 918 kg $m^{-3}$ for meteoric ice.

*Table 1. List of datasets included and source.*

| | Description | Units | Data Sources | References |
|---|---|---|---|---|
| mask | Basic mask, ocean/ice shelf/grounded ice | - | MOA grounding line | Haran et al., 2005, Scambos et al., 2007 |
| mask+ | Ice free/ice stream mask | - | ADD, Jonathan Bamber, Laura Edwards | www.add.scar.org |
| glmask | Grounding line uncertainty mask | - | Anne Le Brocq | This document |
| umask | Mask indicating areas where surface is not consistent with JLB/JAG DEM | - | Anne Le Brocq | This document |
| bmask | Mask indicating sources of bed/bathymetry data | - | Anne Le Brocq | This document |
| usrf | Upper ice surface elevation | m | Jennifer Griggs/ Jonathan Bamber, RAMP | Bamber et al., 2009, Liu et al., 1999 |
| lsrf | Lower ice surface elevation | m | Jennifer Griggs/ Jonathan Bamber, BEDMAP, AGASEA/BBAS | Griggs & Bamber 2009b, Lythe et al., 2001, Vaughan et al., 2006, Holt et al., 2006. |
| topg | Bed/bathymetry elevation | m | BEDMAP, Frank Nitsche | Lythe et al., 2001, Nitsche et al., 2007 |
| lsrf2 | Lower ice surface elevation (including Recovery basin modification) | m | As lsrf, plus Anne Le Brocq | As lsrf, plus Le Brocq et al., 2008. |
| topg2 | Bed/bathymetry elevation (including Recovery basin modification) | m | As topg, plus Anne Le Brocq | As topg, plus Le Brocq et al., 2008. |
| firn | Firn correction | m | Michiel van den Broeke | Van den Broeke et al., 2008 |
| temp | Surface air temperature | °C | Joey Comiso | Comiso, 2000 |
| accr | Accumulation | m (ice equivalent) | Michiel van den Broeke | Van de Berg et al., 2006 |
| acca | Accumulation | m (ice equivalent) | Rob Athern | Athern et al., 2006 |
| ghffm | Geothermal heat flux | mW $m^{-2}$ | Cathrine Fox Maule | Fox Maule et al., 2005 |
| ghfsr | Geothermal heat flux | mW $m^{-2}$ | Nicholas Shapiro | Shapiro & Ritzwoller, 2004 |

## *2. Mask*

### 2.1 'mask'

The basic mask is derived from the MOA (Mosaic of Antarctica) coastline shapefiles (http://nsidc.org/data/docs/agdc/nsidc0280_scambos/), then modified in order to create a smooth join between the grounded and floating ice thickness datasets (see Section 3.1.3). There were a number of iterations where the current mask is used to join the data, the result considered, then the mask modified to ensure the best join. The areas of major change are discussed in Section 2.3 below.

The three shapefiles (coastline, grounding line and islands) provided by MOA were combined into a single shapefile, and converted to a polygon shapefile (using ArcGIS). The three separate files do not overlay exactly which causes problems when gridding the mask from the polygon shapefile. In order to overcome this, polygons with an area smaller than a given threshold (10 $km^2$) were deleted. The result was then checked to ensure that no 'genuine' small polygons were missing, and they were reinstated as necessary. Three islands were found to be completely missing from the original MOA dataset (Smyley Island and Case Island at the western end of George VI Ice Shelf, and Sherman Island incorporated in the Abbott Ice Shelf, see Fig. 1 for locations discussed in the text), these were added by digitising the extent from the original MOA image. Each polygon was then manually assigned a code for ocean, floating ice and grounded ice. The polygon shapefile was then converted to a 5 km grid (Fig. 1) using the ArcMap Spatial Analyst 'convert features to raster' function. It should be noted that this conversion algorithm assigns the value of the polygon at the centre of the grid cell to each each given grid cell. The mask values are given in Table 2.

The mask was then modified to make it 'modelling friendly', i.e. by removing small ice shelves (1 or 2 cells), and islands less than one grid cell wide. The join between the grounded and floating ice datasets was also considered, with small changes made to ensure a smooth join, allowing for one grid cell width smoothing boundary (see Section 3.1.3).

*Table 2. Mask values*

| Mask file | Value | Description |
|---|---|---|
| mask | 0 | Ocean |
| mask | 1 | Grounded ice |
| mask | 2 | Ice shelf |
| mask+ | 0 | Non ice free/ice stream |
| mask+ | 3 | Ice free |
| mask+ | 4 | Ice stream (> 250 m $yr^{-1}$) |
| glmask | 0 | Non 'ice plain' |
| glmask | 5 | 'Ice plain' |

### *2.2 'mask+'*

The purpose of the 'mask+' mask is to provide extra information, in addition to that provided in the basic mask. It indicates terrestrial regions that are currently ice free and ice stream regions, here defined by velocities over 250 m $yr^{-1}$.

#### *2.2.1 Ice free areas*

The ice free regions were derived from the ADD (Antarctic Digital Database) 'rock' polygon coverage. The polygon coverage was first converted to a 1 km grid (rock/no rock), then converted to a 5 km grid based on the number of subcells which were ice free (rock). A threshold of 33 % of the subcells being ice free was chosen for ice free cells at 5 km, based on the resulting 5 km mask. Hence the 5 km ice free mask does not include all areas which are ice free, only those which cover a certain area.

#### *2.2.2 Ice stream areas*

The ice stream regions were derived from a combined map of InSAR velocities, (Edwards, 2008). The InSAR velocity map does not cover all regions, hence some ice streams locations have here been supplemented by balance velocities. The mask only includes the 'major' ice streams, some small outlet glacier are not coherent enough at a 5 km resolution, so have not been included (Fig. 1). Therefore the mask should only be considered indicative rather than definitive.

**2.3 'glmask'**

The glmask delineates differences between the ADD coastline polygon, the MOA polygon and the final mask provided in this dataset (Fig. 1). Hence, it delineates areas where there is some uncertainty in the grounding line location, i.e., areas where it is likely that there is an ice plain (an area where the ice is close to grounding/flotation). The original MOA grounding line is derived from the 'break of slope', rather than the grounding line. In ice stream grounding zone areas, it is difficult to define a grounding line as such, and it is not the 'break of slope', hence, the MOA mask is often a long way (10s km) inland from where it is believed to be (notably Pine Island Glacier, Slessor Glacier). The ADD grounding line is perhaps more reliable in some ice stream regions (though generally much less reliable than MOA).

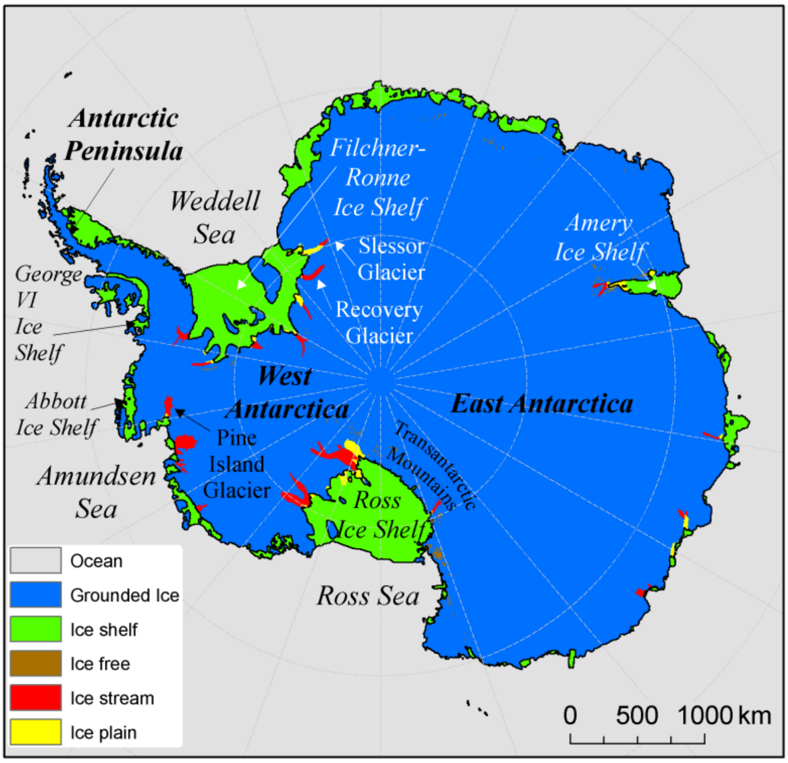


*Figure 1. Combination of mask, mask+ and glmask.*

***3. Ice sheet configuration***

As mentioned in the introduction, the BEDMAP dataset provides information on the bed topography, bathymetry and ice thickness. However it contains a large number of inconsistencies, (e.g. bed + thickness not equal to measured surface) and when a flotation calculation is carried out, does not provide a grounding line consistent with observations. It is the aim of this section to produce a dataset that is free of these inconsistencies, suitable for initialising a numerical model for the present day ice sheet configuration. The following discussion outlines the important factors which need to be considered.

- It is critical that if the mask indicates the ice is grounded, then it is grounded and likewise for floating ice. BEDMAP has a large number of ice shelf areas which become grounded due to poor sub-ice shelf interpolation. If the ice surface is derived by adding the ice thickness to the basal topography in areas which become grounded, then this will introduce a large number of spurious grounded 'islands' into the ice shelf areas.
- Around ice stream grounding zones, it is important that no modifications affect the ice sheet surface, e.g. changing the ice shelf thickness will change the resulting ice surface from a flotation calculation. The ice surface derived from any flotation calculation must be consistent with the measured surface, hence, here the ice thickness in the ice shelf areas is derived from the ice surface and a firn correction. Any flotation

calculation must include the firn correction and use the densities given here to ensure the ice sheet surface remains consistent. Otherwise, spurious bumps will appear, which will be highly noticeable in low slope ice stream regions.

- It is also important that there are no false or large gradients in the ice surface, thickness or bed/bathymetry, as can arise when a number of datasets are combined. The consequence of this would be unfeasibly large gravitational driving stress (and hence velocities).

Fig. 2 shows a flow diagram which works through the procedure that has been carried out in the data preparation. The overall procedure consists of 7 steps which are documented further below. Firstly, the grounded and floating ice thickness datasets are joined, and the boundary smoothed to provide a smooth join. Then a combined ice sheet surface is created, from two different DEMs (Digital Elevation Models). Next, the grounded ice sheet bed is derived from this surface and the combined thickness dataset. A check is then carried out to ensure that the ice is entirely grounded. All the bathymetry datasets are then merged, the join smoothed in some regions, then a flotation check is carried out, and grounded areas excavated.

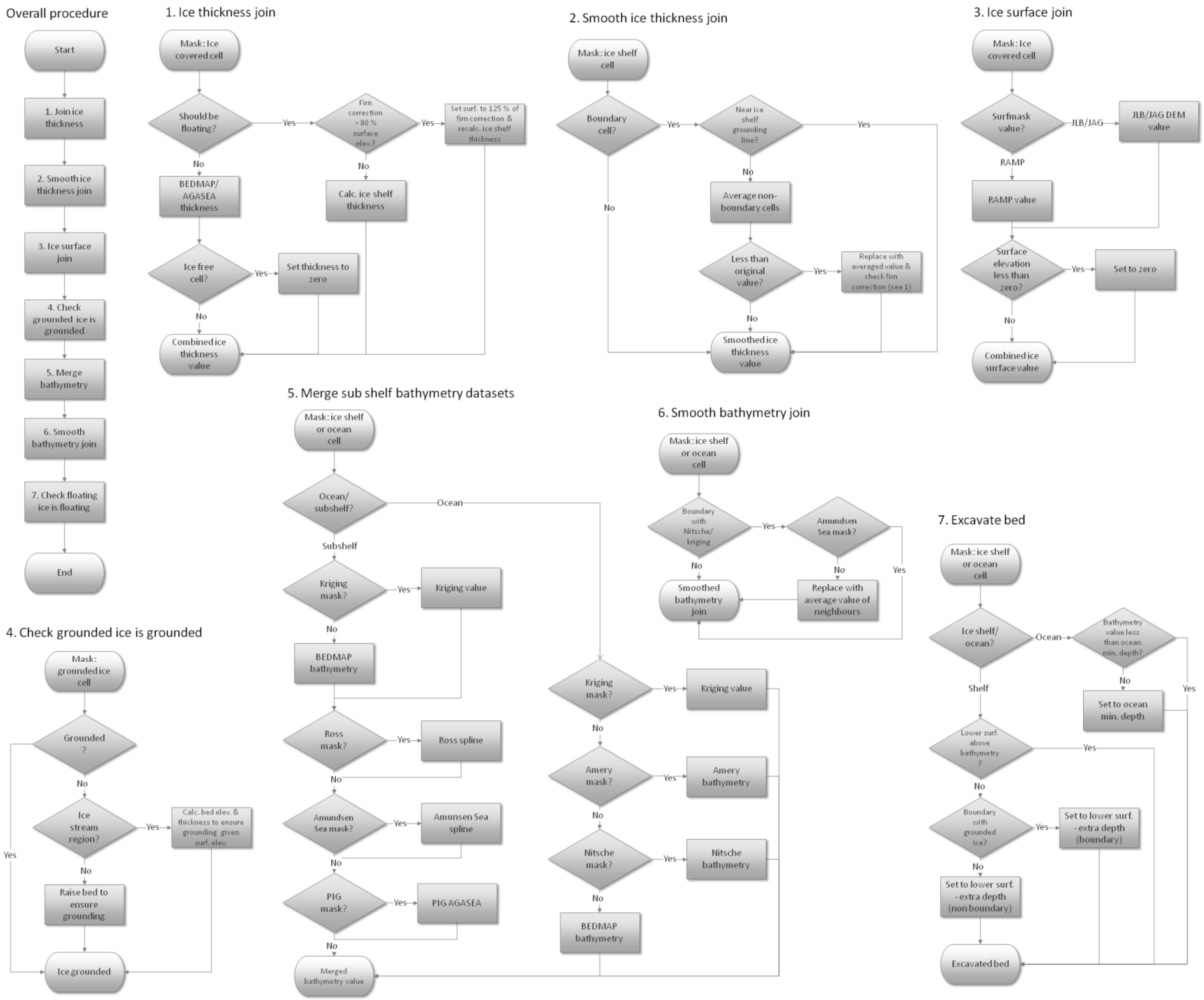


*Figure 2. Flow chart describing data processing*

### *3.1 Ice thickness*

This section describes the merging of various sources of ice thickness data. Firstly, the merging of two grounded ice datasets is described (Section 3.1.1), then the merging of the grounded ice thickness with the floating ice shelf thickness is described (Section 3.1.2).

#### *3.1.1 Grounded ice*

Two versions of the ice thickness were produced, both with (leading to lsrf2 and topg2, see Table 1) and without (lsfr and topg) the Recovery Glacier region inferred ice thickness of Le Brocq et al., (2008). Aside from this, two sources of ice thickness data are merged: the original BEDMAP ice thickness (Lythe et al., 2001) and the AGASEA/BBAS Amundsen Sea data (Vaughan et al., 2006, Holt et al. 2006).

The AGASEA/BBAS ice thickness data for the Amundsen Sea region was downloaded from: http://www.ig.utexas.edu/research/projects/agasea/agasea_results.htm and joined to the BEDMAP ice thickness dataset (http://www.antarctica.ac.uk//bas_research/data/access/bedmap/) as follows.

Firstly, the BEDMAP ice thickness was smoothed using a low pass filter (3x3 window), to remove spurious patterning present. It should be noted that the original bed elevation dataset from BEDMAP is smooth in comparison to the ice thickness, so must have been smoothed at some point in the preparation of the dataset.

The region where there is dense coverage of RES flight lines in the AGASEA/BBAS dataset was identified, and the two datasets masked with a buffer zone where the two datasets overlap (shown in Fig. 3). The buffer zone has a width of 30 km. In the buffer zone, the two ice thickness grids were averaged and then the values (including one cell width border outside of the buffer zone) smoothed using a low pass filter to ensure a smooth join in the final dataset.

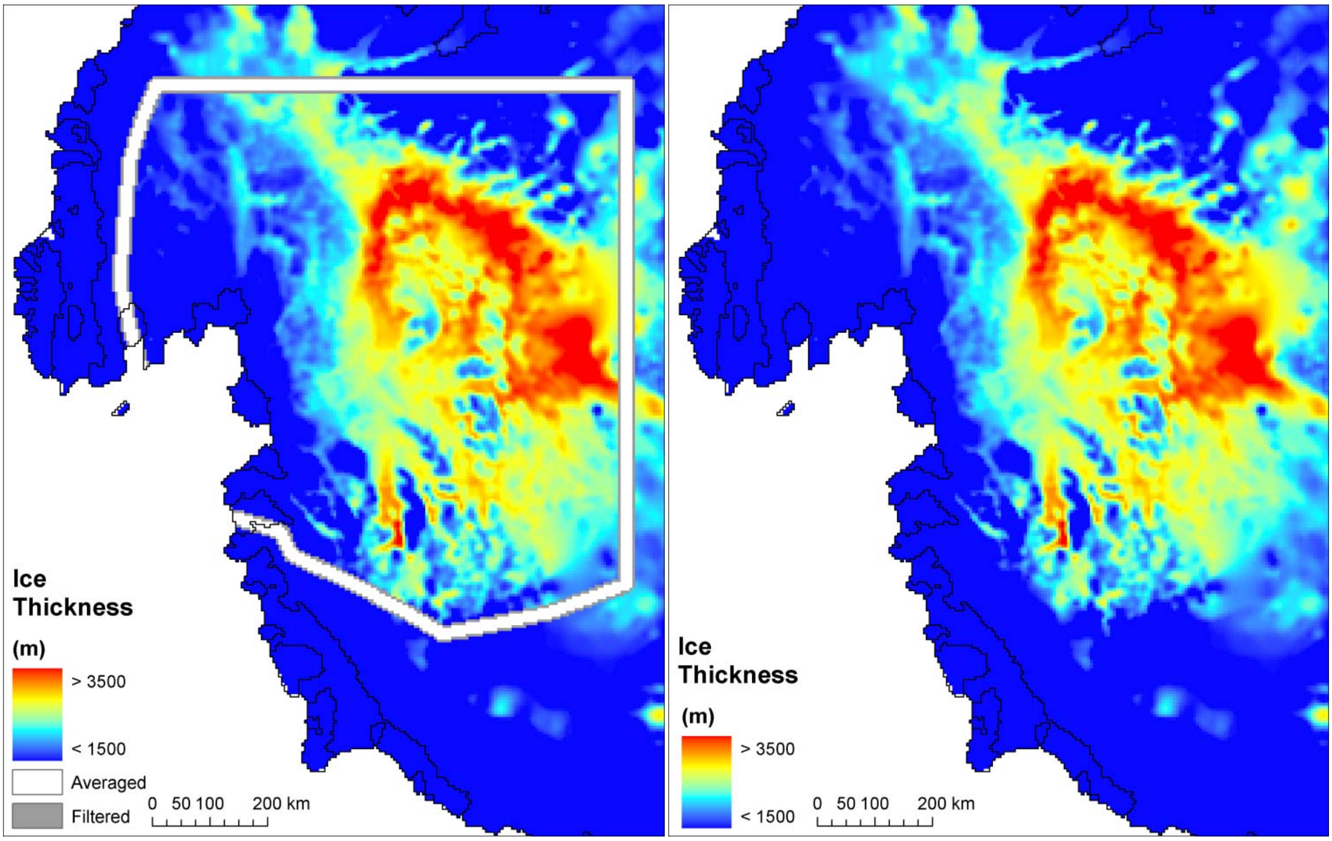


a) b)

*Figure 3. a) White area is averaged area (buffer zone), b) joined dataset. (Black line is outline of mask)*

For lsrf2 and topg2, the Le Brocq et al. (2008) ice thickness was merged with the BEDMAP data in the same way as the AGASEA/BBAS dataset.

The ice thickness at ice free locations, according to mask+, were set to zero. The ice thickness in areas which should be ice covered according to mask+, but were ice free, was calculated as an average of their ice covered neighbours (umask value 7, see Section 3.6). If a location has no ice covered neighbours, the ice thickness was set to 50 m (umask value 8, see Table 3).

### *3.1.2 Floating ice*

Many ice shelves around Antarctica do not have measurements of ice thickness available for them. The BEDMAP dataset used a hydrostatic assumption to derive ice shelf thickness from surface elevations measured from satellite altimetry (see Fig. 4a for BEDMAP ice thickness). Since then, however, a newer surface DEM has become available, incorporating IceSat laser altimetry data, as well as radar altimetry (Bamber et al., 2009). In order to calculate the ice shelf thickness from the surface elevation, the respective densities of ocean water and ice need to be specified and an estimate of the depth and density of the firn layer is also required. Since the BEDMAP dataset was compiled, a spatial estimate of the firn correction for Antarctica has been produced using a regional climate model (Van den Broeke et al., 2008, Fig. 5). Therefore, the ice shelf thickness has been recalculated for the dataset presented in this paper.

The firn correction data were gridded in the same way as the Van de Berg et al. (2006) accumulation data, see Section 5.1 for more details. Beyond the continental shelf, a value of 16.5 m is applied, which is the average ice shelf firn correction value.

Following Griggs and Bamber (2009a), the equivalent ice thickness ($H_i$ , corresponding to the ice thickness if all the ice column was at the density of meteoric ice) is given by

$$H_i = \frac{(s-f)\rho_{\mathrm{w}}}{\rho_{\mathrm{w}} - \rho_{\mathrm{i}}}, \tag{1}$$

where $s$ is elevation above sea level, $f$ is a firn correction (defined as the difference between the actual depth of the firn layer and the depth that the firn would be if it was all at the density of meteoric ice), $\rho_{\mathrm{w}}$ is the density of sea water, $\rho_{\mathrm{i}}$ is meteoric ice density. The actual ice thickness ($H$) is, therefore, the equivalent ice thickness ($H_{\mathrm{i}}$) plus the firn correction ($f$),

$$H = H_i + f\,, \tag{2}$$

and, hence,

$$H = \frac{(s-f)\rho_{\mathrm{w}}}{\rho_{\mathrm{w}} - \rho_{\mathrm{i}}} + f\,. \tag{3}$$

It is the actual ice thickness ($H$), i.e. meteoric ice thickness plus firn thickness, which is incorporated into the dataset. Any flotation calculation in an ice-sheet model should incorporate the firn correction in the calculation.

Eqs. 1 & 3 assume a constant density for ocean water (1028 kg $m^{-3}$) and ice (918 kg $m^{-3}$). In areas where surface melt occurs the firn correction is likely to be overestimated (Griggs and Bamber, 2009b, Michiel Van den Broeke pers. comm.), however this is unlikely to affect the major ice shelves.

In some areas the firn correction is greater than the surface elevation, generally around the periphery of ice shelves where there is a high degree of uncertainty in the surface elevation, or uncertainty whether there is actually shelf ice present at all. Where the firn correction is greater than 80 % of the surface elevation, the surface elevation is set to 125 % (100 / 0.8) of the firn correction value, and the ice shelf thickness calculated from this surface. These areas are indicated in umask (value of 4).

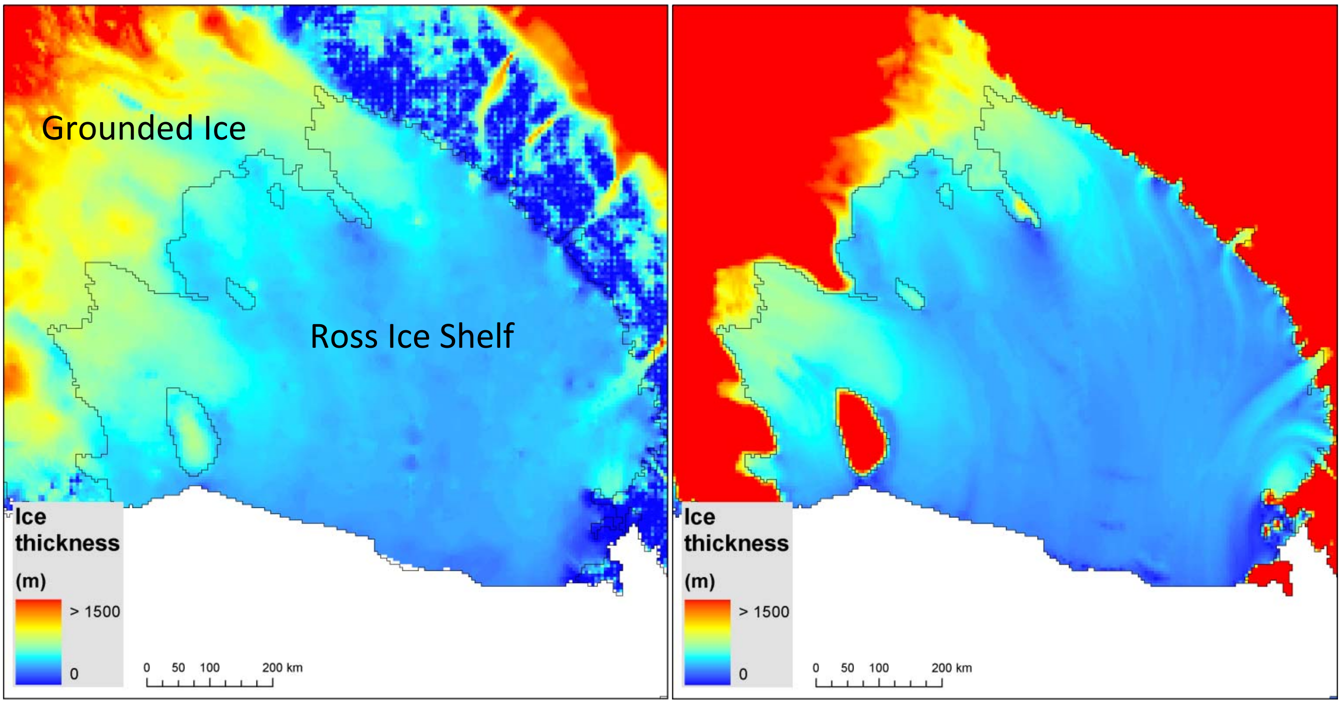


*a)* *b)*

*Figure 4 . a) BEDMAP ice thickness, b) ice thickness (this dataset) calculated from surface DEM and a flotation calculation (note that ice thickness calculation is not valid in grounded areas, however, it is shown here for completeness, black line is outline of mask)*

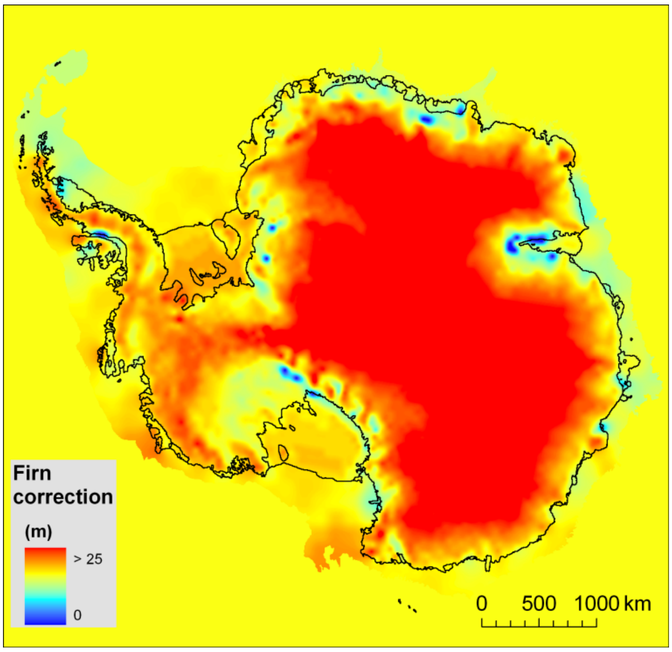


*Figure 5. Firn correction (black line is outline of mask).*

### ***3.1.3 Joining ice thickness datasets***

The grounded ice thickness and the ice shelf thickness must be joined smoothly to avoid any steep gradients in ice thickness. However, in order to maintain the consistency between the ice thickness and the upper ice surface in the ice shelf regions, the ice thickness cannot be smoothed in grounding line regions of the major ice streams. Hence, there is no smoothing carried out across the major ice stream grounding lines in the dataset presented here.

Away from the major ice stream grounding lines, the break in slope at the grounding line is more obvious, and the surface DEM is less reliable due to 'loss of lock' in the radar altimetry data (Griggs and Bamber, 2009). This leads to a 'contamination' of the surface heights in ice shelf regions close to the grounding line, and causes larger errors in the surface elevation and hence potentially elevated ice thicknesses. Ice thickness values in ice shelf cells that are on a border with the grounded ice were smoothed (average of 'non-border' neighbours). The original value was then replaced with the smoothed value if the smoothed value was less than the original. This removes the spuriously high ice thickness values introduced at the grounding line by errors in the surface DEM (see Fig. 6). A similar check to that in section 3.1.2 was carried out to make sure that the smoothed ice thickness values were sufficient to lead to a surface elevation value greater than 125 % of the firn correction.

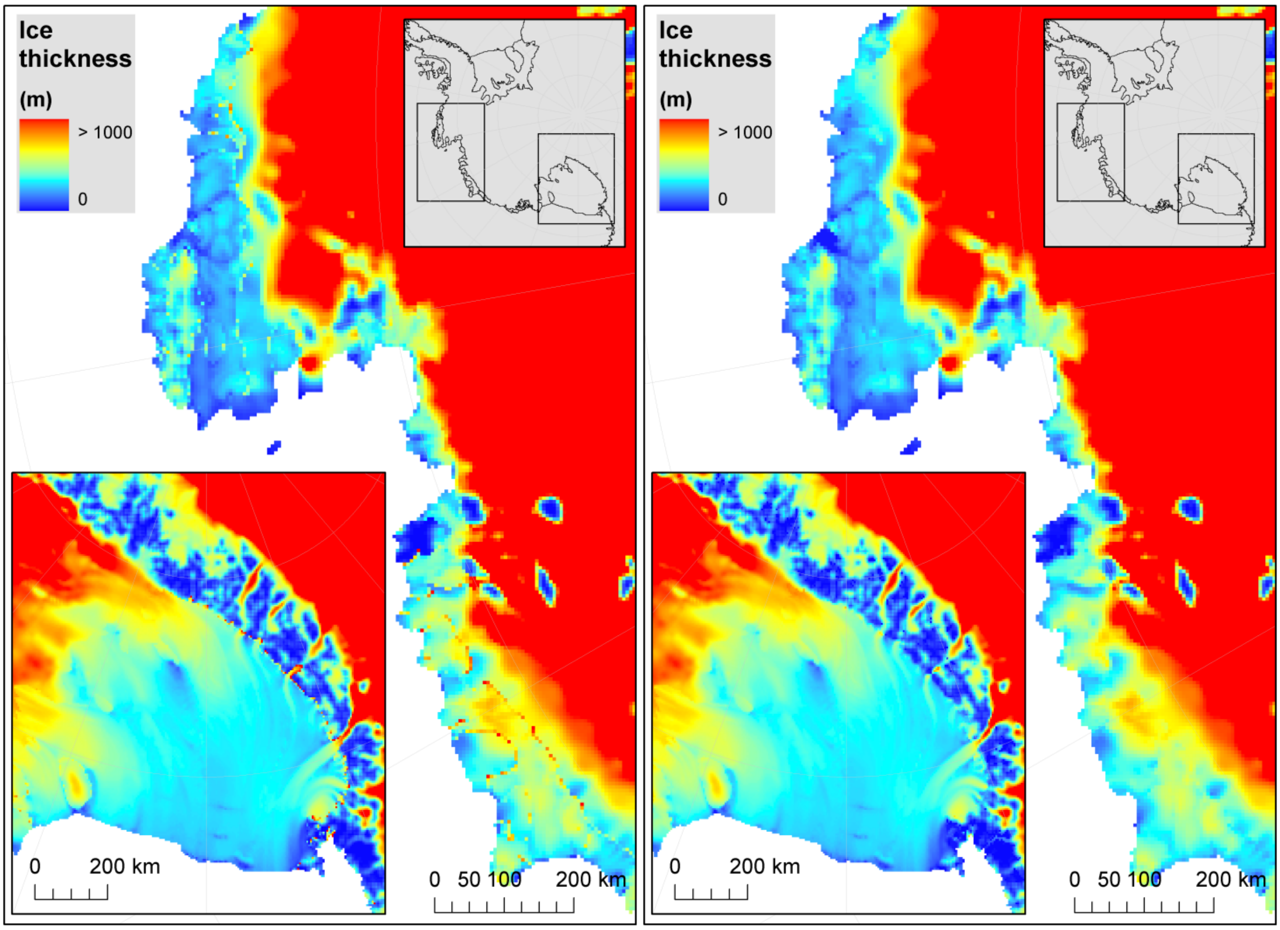


*a)* *b)*

*Figure 6. a) Pre-smooth join and b) smoothed join.*

***3.2. Ice surface***

This section describes the ice surface DEM. The DEM is largely derived from the DEM of Jonathan Bamber and Jennifer Griggs (JLB/JAG DEM), however there are some modifications made at this stage and at a later stage for the final ice sheet surface (see the description of umask in Section 3.6). Initially the DEM is a combination of the JLB/JAG DEM (non-Antarctic Peninsula) and the RAMP DEM (Antarctic Peninsula). The JLB/JAG DEM is derived solely from radar and laser altimetry, hence, the coverage is sparse over the Antarctic Peninsula and the DEM does not look realistic (Fig. 7a). The RAMP DEM incorporates ADD data over the Antarctic Peninsula, and whilst this also has large inherent errors, is probably more accurate than the JLB/JAG DEM. The two were combined in grounded ice regions only, using the mask shown in Fig. 7. The version of the JLB/JAG DEM used in the dataset presented here differs slightly from the published version, using a tension spline interpolation technique instead of kriging. The tension spline version is smoother, but may miss some high resolution spatial features.

At this stage, the ice surface DEM is used, in combination with the ice thickness, to calculate the bed elevation in grounded areas of the ice sheet. Later, the surface elevation is re-calculated for ice shelf regions, and will differ from the original DEM, due to the ice thickness smoothing that occurred in Section 3.1.3. Small areas of the ice surface DEM, in grounded regions, are artificially raised in the next section, however these are not in ice stream regions, and generally are in areas where the DEM error is high.

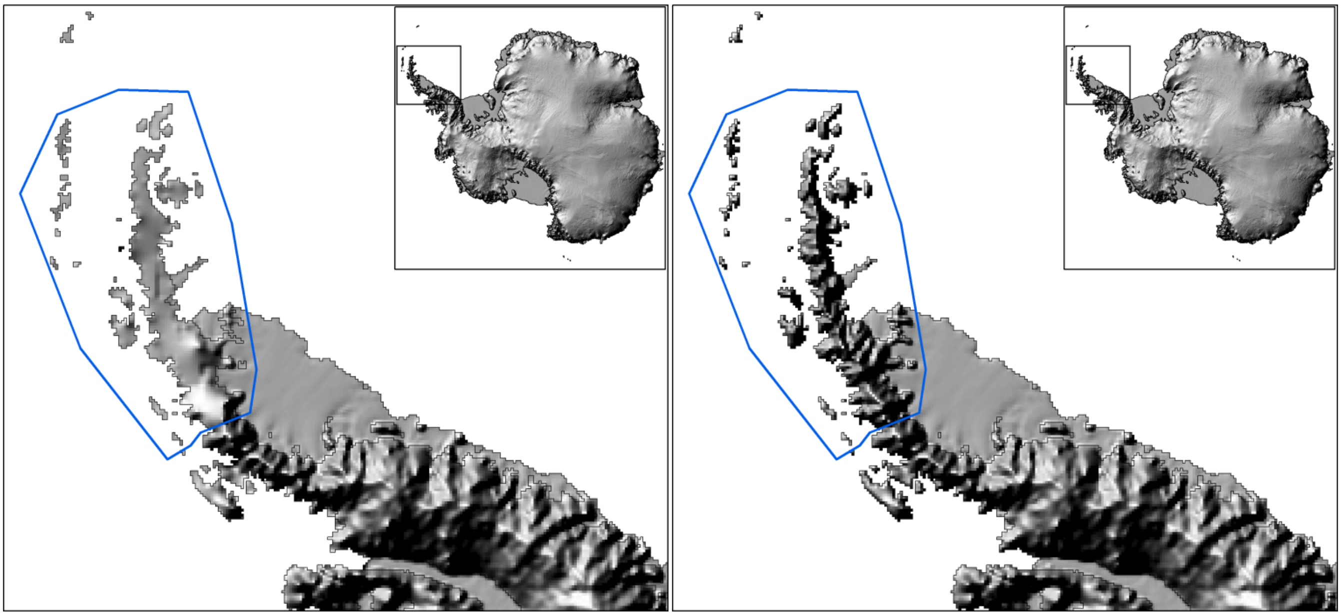

*a)* *b)*

*Figure 7. Antarctic Peninsula DEM; a) hillshade of original JLB/JAG DEM, b) hillshade of combined surface DEM (after the bed was raised in non grounded regions – see Section 3.3, black line is outline of mask, blue line is RAMP data extent).*

### *3.3. Grounded ice covered bed elevation*

The bed elevation in the grounded ice region was derived by subtracting the grounded ice thickness (Section 3.1.1) from the combined ice surface dataset (Section 3.2). The ice thickness above buoyancy ($H^*$) was calculated using

$$H^* = (H - f) + (\rho_w / \rho_i) h \,, \tag{4}$$

where $h$ is bed elevation, and checked to ensure that the ice is grounded (where $H^* \geq 0$). There are two different areas where this may not be the case and these are treated separately:

1) where the ice surface / thickness is not confidently known, and away from major ice stream grounding lines. In these areas the bed elevation is increased to ensure the ice is grounded, hence the ice surface elevation is altered. These areas are indicated with a value of 4 in umask (see Section 3.6), there are 544 grid cells which are altered, around 0.1 % of the grounded ice cells.

2) ice stream areas, where it is important to keep the ice surface elevation the same as the DEM. In these regions the bed elevation and thickness needed to cause grounding, with the surface elevation from the surface DEM, is calculated by rearranging Eq. 4 in terms of the actual ice thickness ($H$) and surface elevation ($s$),

$$H = \frac{H^* + f - (\rho_w / \rho_i)s}{1 - (\rho_w / \rho_i)}, \tag{5}$$

where $H$* here is set to 1 m.

The bed elevation ($h$) is then derived from

$$h = s - H\ . \tag{6}$$

Ice free areas (see mask+) were checked to ensure their elevation was above sea level, and their elevation set to a given elevation (10 m) if not.

### *3.4. Sub-ice shelf bathymetry*

Away from the main ice shelves, there are very limited data on the sub-ice shelf bathymetry. In BEDMAP, the interpolation algorithms used led to bathymetry values which did not allow the ice shelf to actually float. This section describes the various methods used to reinterpolate various areas of sub-ice shelf bathymetry. It should be emphasised here that the BEDMAP gridded datsets have been used for the reinterpolation, rather than the original BEDMAP database of measurements. The most straightforward method to ensure the ice shelves float would be to simply excavate a certain depth beneath the lower surface of the ice shelf, however this would lead to a uniform cavity depth, and this would not be realistic. The approach taken here is to carry out a slightly 'supervised' approach to the reinterpolation, identifying the problem areas, and tailoring the interpolation methods to each area. The bathymetry still requires excavation in certain areas, this is described in Section 3.4.6. The following sections describe the interpolation procedures for different areas: small ice shelves around East Antarctica (Section 3.4.1), the Ross Ice Shelf near the Transantarctic Mountains (Section 3.4.2), the Amundsen Sea region (Section 3.4.3), Pine Island Glacier (PIG) sub-ice shelf (Section 3.4.4) and the Amery sub-ice shelf region (Section 3.4.5).

It should be noted that the original BEDMAP bathymetry was on a slightly different coordinate reference than the BEDMAP ice thickness. When comparing the bathymetry with other datasets, it also appeared to be slightly offset. As a result, the BEDMAP bathymetry was shifted by -3134 m in the x direction and 1866 m in the y direction to remove this apparent shift.

#### *3.4.1. General bathymetry - Kriging*

The bathymetry in BEDMAP beneath the small ice shelves fringing the ice sheet (see red outline in Fig. 8) is very shallow. Therefore, the bathymetry in these regions was reinterpolated, however the reinterpolation is not applied where the mask overlies the major ice shelves (Ross/Filchner Ronne/Amery), as these are better constrained by observation, or for ice shelves in the Amundsen Sea region, which are reinterpolated using a different method (see Section 3.4.3).

All ice shelf areas within the red outline shown on Fig. 8 were set to nodata, also, where the ocean bathymetry elevations were higher than -300 m, the elevation was set to nodata. The nodata values were then reinterpolated (using both grounded bed and bathymetry < -300 m) using kriging to produce deeper bathymetry (see Fig. 8).

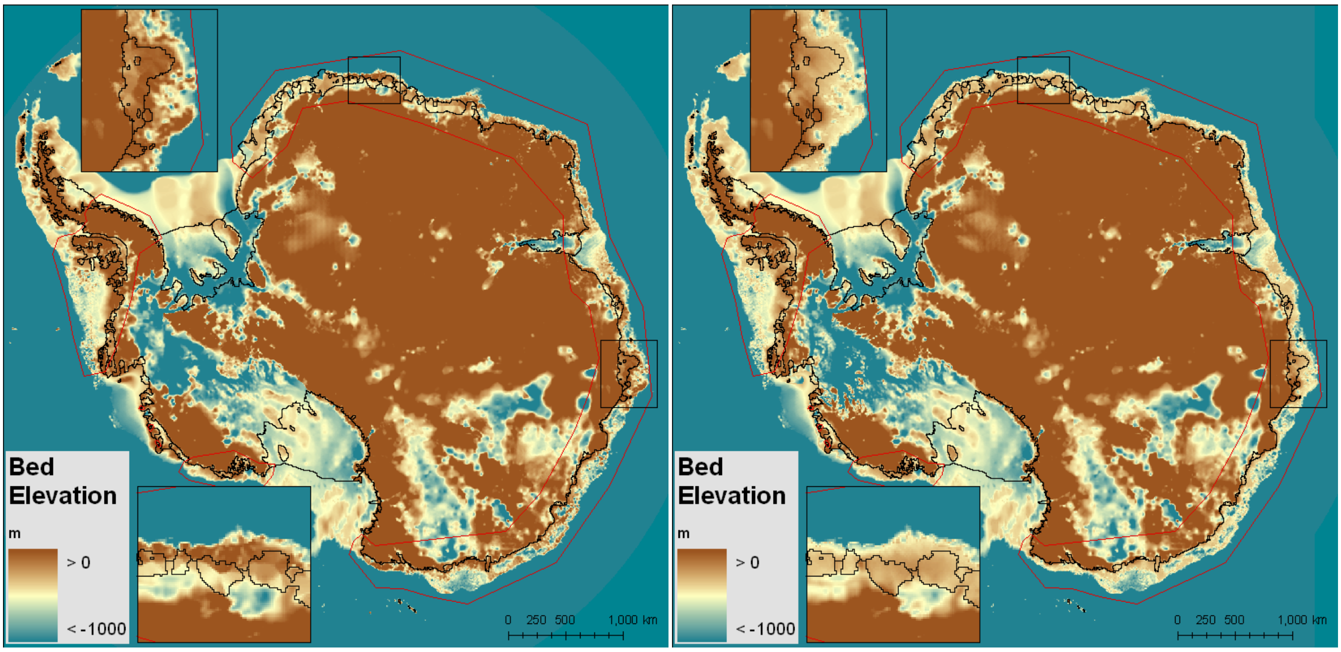


*a) b)*

*Figure 8. a) Original BEDMAP, b) modified BEDMAP, reinterpolation where bathymetry > -300 m (black line is outline of mask).*

### *3.4.2. Ross Ice Shelf*

Near the Transantarctic mountains, beneath the western Ross Ice Shelf, there is very little data available on the bathymetry. As a result, in combination with the Inverse Distance Weighting (IDW) interpolation used in BEDMAP, there is some 'leakage' of the high elevations into the sub-ice shelf region. This could be avoided using a spline interpolation technique, which would take into account the steep slope of the mountains towards the sub-ice shelf region, into the deep sub-ice shelf bathymetry. The most erroneous area was identified by eye (see red outline on Fig. 9a) and set to nodata in the sub-ice shelf region. The area was then reinterpolated using a tension spline with a high weighting and high number of points in order to force the sub-ice shelf region near to the mountains to have a steep elevation gradient, into a deep, lower gradient surface away from the mountains (see Fig. 9b).

### *3.4.3. Amundsen Sea*

Since BEDMAP was created, a large amount of new bathymetry data has become available for the Amundsen Sea region, these data were compiled by Nitsche et al. (2007) (see Section 3.5.1). These bathymetry data are useful for re-interpolating the Amundsen Sea sub-ice shelf bathymetry, as it provides new information on the bathymetry near ice shelf fronts. In order to utilise this, the data was combined with the grounded ice sheet bed from Section 3.3 and the BEDMAP bathymetry beyond the Nitsche dataset. The sub-ice shelf regions were then set to nodata.

The Nitsche bathymetry suggests that the sub-ice shelf bathymetry in the Amundsen Sea is reasonably deep, with 'trough' like features in the sub-ice shelf regions (see Fig. 10). As with the Ross Sea bathymetry (Section 3.4.2), this morphology lends itself to spline interpolation. However, away from the ocean bathymetry data, even spline interpolation may lead to too shallow sub-ice shelf bathymetry and cause the ice shelves to ground.

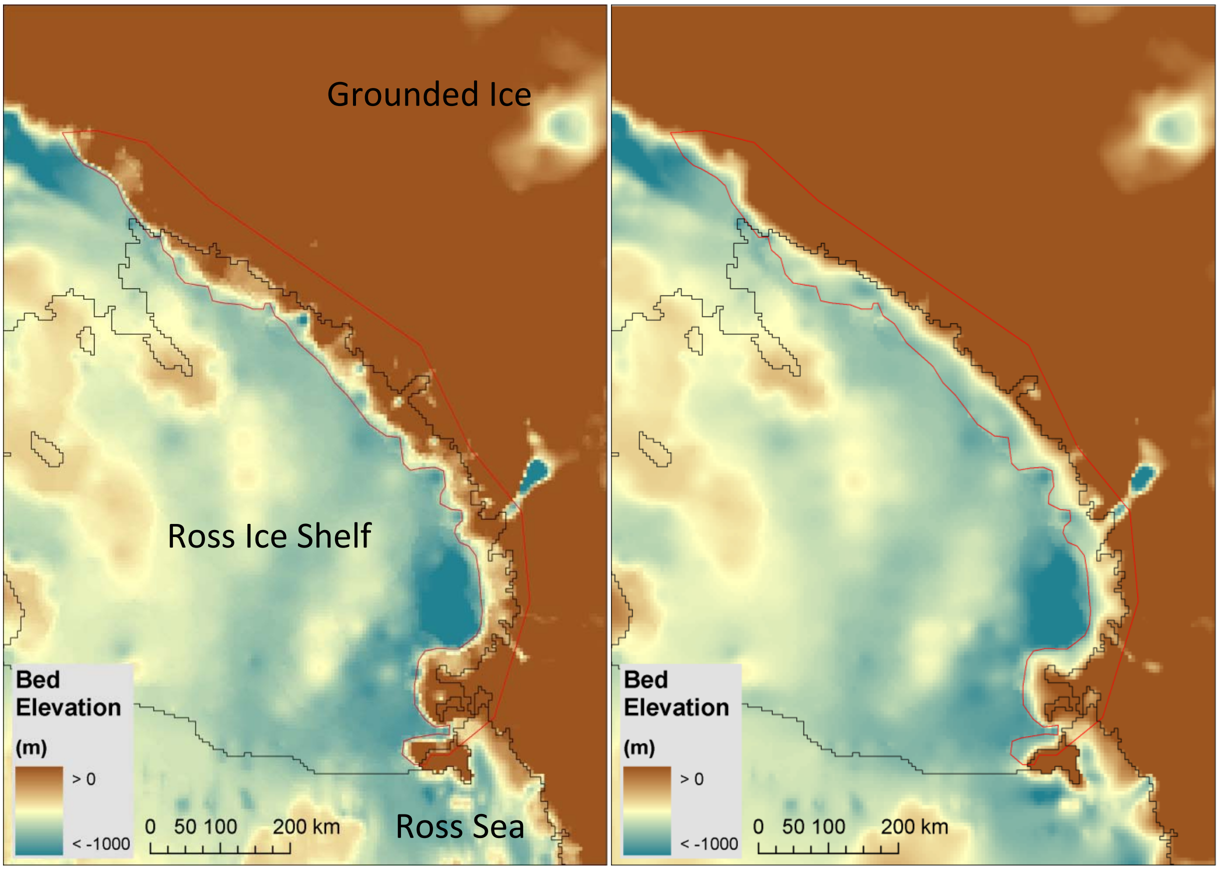


*a)* *b)*

*Figure 9. Ross Ice Shelf bathymetry; a) Original BEDMAP, b) spline interpolation (ice shelf area within red outline), (black line is outline of mask).*

Therefore, in order to aid the interpolation process, the 'bottom' of the troughs was imposed as a function of the ocean bathymetry at one end of a transect, and the grounded ice bed elevation at the other. A series of transects were constructed (Fig. 10b) and the sub-ice shelf bathymetry value, along the transect, calculated as a linear function of distance from either the ocean end of the transect, or the grounded ice sheet end. These values were then combined with the masked bed/bathymetry data outside of ice shelf areas, and a spline interpolation carried out (Fig. 10c). The result is very different from BEDMAP, and leads to deep sub-ice shelf cavities around the Amundsen Sea (compare Fig. 10a & c).

Originally a transect was drawn connecting both ocean ends of the Getz Ice Shelf (see Fig. 10a), leading to a large deep trough beneath the ice shelf. However, after subsequent conversations with Ralph Timmerman, and indirectly with Stan Jacobs, this was revised, as it was felt that there was no evidence of throughflow, in oceanographic data from the area. Where two transects join as beneath the Getz sub-ice shelf, the transect connected to both the ocean and grounded bed is interpolated first, then the connecting transect uses the newly interpolated value at its connected end.

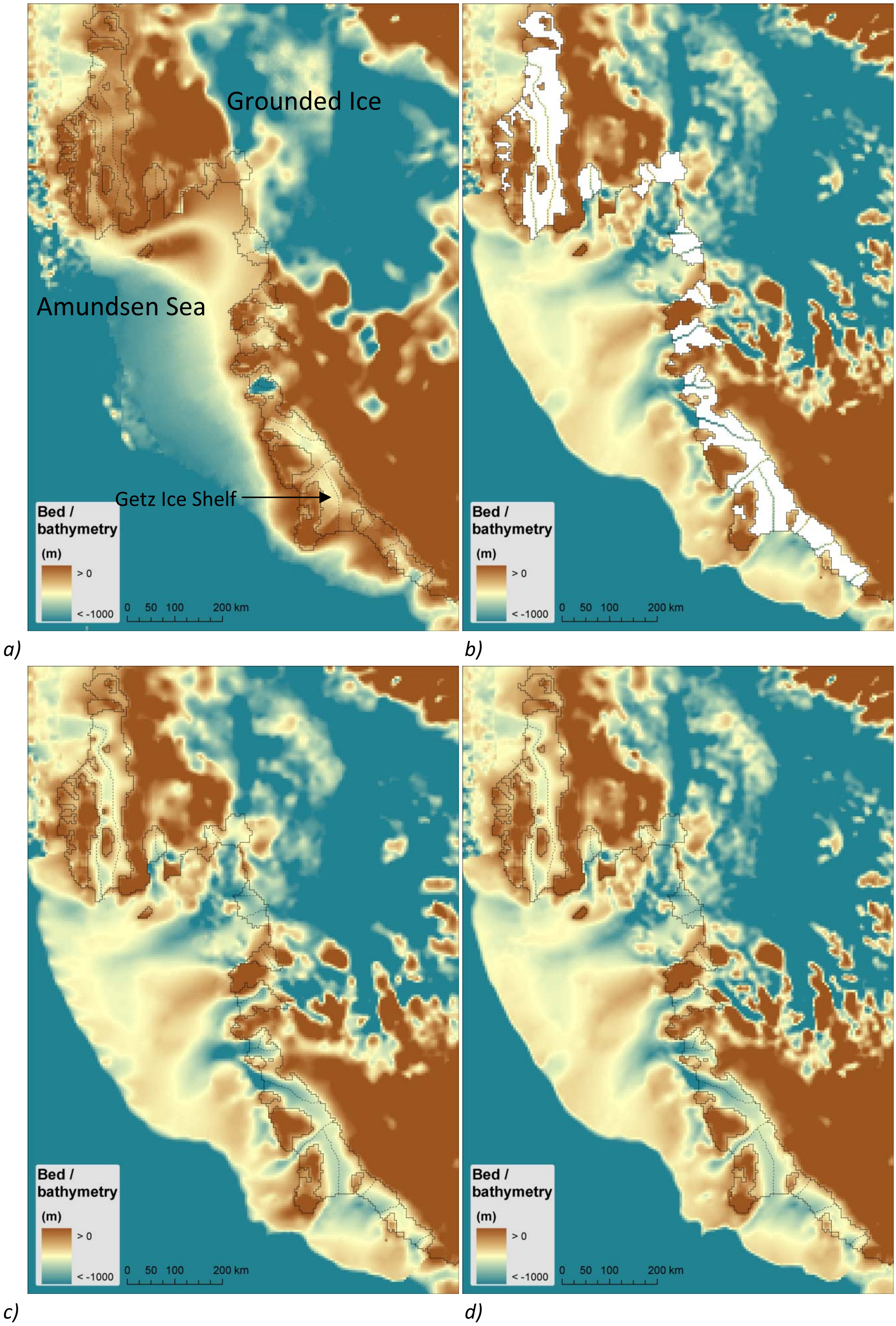


*Figure 10. Amundsen Sea bathymetry; a) original BEDMAP bed and bathymetry, b) data used in spline interpolation, c) resulting interpolation (note PIG sub-ice shelf altered later in Section 3.4.4), d) final bed / bathymetry including PIG sub-ice shelf data and excavation (see Section 3.4.6). Solid black line is outline of mask, dashed line is transects described in text.*

### *3.4.4. PIG Ice Shelf*

Part of the PIG sub-ice shelf is treated differently to the rest of the Amundsen Sea ice shelves. Directly in front of PIG itself, there is a trench connecting the ocean with the base of the ice stream. Rather than simply linearly interpolating the trench as in Section 3.4.3, the original AGASEA data are used solely in the 'trench' (see Fig.10d).

### *3.4.5. Amery Ice Shelf*

Whilst there is some data for the sub-ice shelf bathymetry in the Amery region in BEDMAP, there is also a large area that is based on interpolation. This led to a 'ridge' appearing which has hampered numerical modelling attempts for this region previously (Philippe Huybrechts pers. comm.). Recent data suggests that this ridge does not exist (Ralph Timmerman, pers. comm.), hence some reinterpolation has been carried out in this work. All bathymetry (sub-ice shelf and ocean) in BEDMAP which was above -600 m was reinterpolated using kriging, and replaced in the masked area shown on Fig. 11c (red outline), chosen to ensure a smooth join between the other datasets.

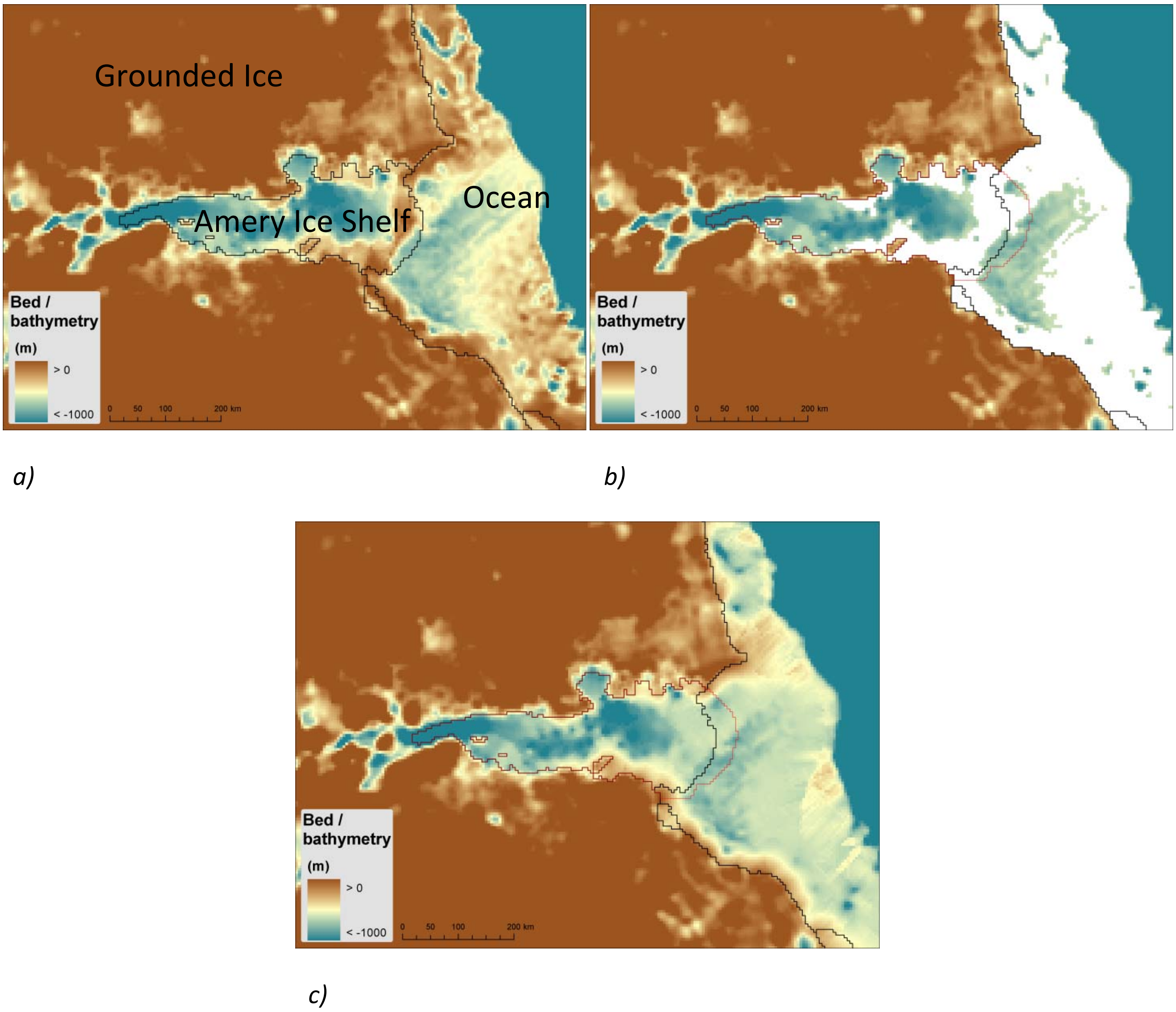


*Figure 11. Amery Ice Shelf bathymetry; a) Original BEDMAP, b) data excluded from reinterpolation and c) reinterpolated (kriging) bathymetry, red line shows the bathymetry area that will be replaced. Note: this does not include the further modifications to the ocean bathymetry (see Section 3.5) or any excavation that occurs in Section 3.4.6.*

***3.4.6. Excavation***

In order to ensure that all the ice shelf regions will be floating, the bed was excavated in areas where the lower ice surface was below the bathymetry elevation (and the extra depth, see below) using

$$h = s - H - d\,, \qquad (7)$$

(where $s$ has been recalculated using the smoothed ice thickness (using Eq. 3)), for cells not in proximity to grounded ice, where $d$ is extra depth specified beneath the ice shelf (20 m, see Table 3) and

$$h = s - H - d_{gl}\,, \qquad (8)$$

for cells with on a boundary with grounded ice, where $d_{gl}$ is extra depth specified beneath the ice shelf next to grounding lines (1 m, see Table 3).

*Table 3. Summary of values used in the processing*

| Description | Value |
|---|---|
| Meteoric Ice density ($\rho_i$) | 918 kg $m^{-3}$ |
| Ocean density ($\rho_w$) | 1028 kg $m^{-3}$ |
| Excavation extra depth ($d$) | 20 m |
| Excavation extra depth (next to grounding line, $d_{gl}$) | 1 m |
| Minimum ice thickness above buoyancy | 1 m |
| Default ice thickness where should be ice covered, but no ice covered neighbours | 50 m |
| Minimum ocean depth | -10 m |
| Minimum ice free surface elevation | 10 m |

***3.5. Ocean bathymetry***

The ocean bathymetry (excluding sub-ice shelf areas) is largely the same as BEDMAP except in two areas, the Amundsen Sea and in continental shelf areas as described in Section 3.4.1. This section describes the processing carried out in these regions.

***3.5.1. Nitsche***

The BEDMAP bathymetry contains very few data from observations in the Amundsen Sea region. The bathymetry dataset of Nitsche et al. (2007) is based on recent ship-based observations and provides a great improvement in the Amundsen Sea region. The lat-lon data was downloaded from:

http://www.marine-geo.org/tools/search/entry.php?id=Amundsen_Sea:Bathymetry_Nitsche

The data were then reprojected onto the polar stereographic grid and interpolated onto the 5 km grid (see Fig. 14b for the result).

***3.5.2. Kriging***

There are many ocean regions bordering with ice shelves (particularly in the East AIS) which have elevations close to sea level (see Fig. 8). This is not appropriate and could pose a major problem for the application of ice sheet models as, if the ice shelf fronts were to advance they would simply ground on these shallow regions. There is very little data for the ocean bathymetry in these regions, hence, it is reasonable to carry out the same interpolation procedure as in the sub-ice shelf section (Section 3.4.1).

### *3.5.3. Final checks*

In the Antarctic Peninsula region, a several ocean areas which should be below sea level, are, in BEDMAP, above sea level, but were not reinterpolated in Section 3.5.2. Any ocean regions that have elevations above -10 m where set to -10 m (umask value 14, see Section 3.6).

### *3.6. Summary of configuration datasets*

Figures 12 & 13 summarise the processing which has been carried out on the ice sheet configuration datasets. This information is provided in umask (upper surface mask) and bmask (bed/bathymetry mask), Tables 4 and 5 below detail the values provided in these masks.

Figure 14 shows both the original BEDMAP bed/bathymetry dataset (Fig. 14a) and the new bed/bathymetry dataset (Fig. 14b). The figure also shows the ice thickness above buoyancy (following Eq. 4) for the original BEDMAP ice sheet configuration (Fig. 14c) and for the new dataset (Fig. 14d).

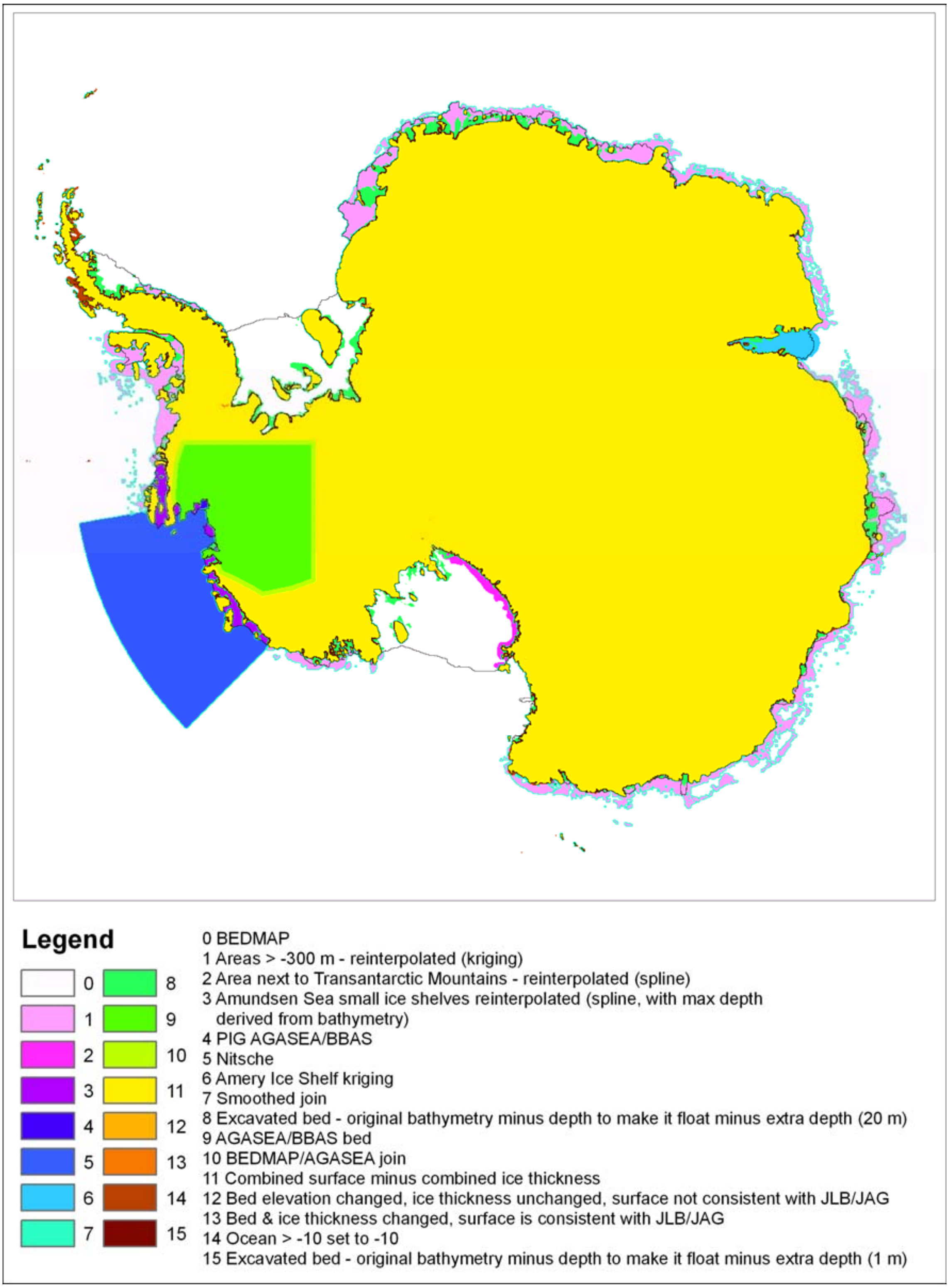


*Figure 12. Description of bmask*

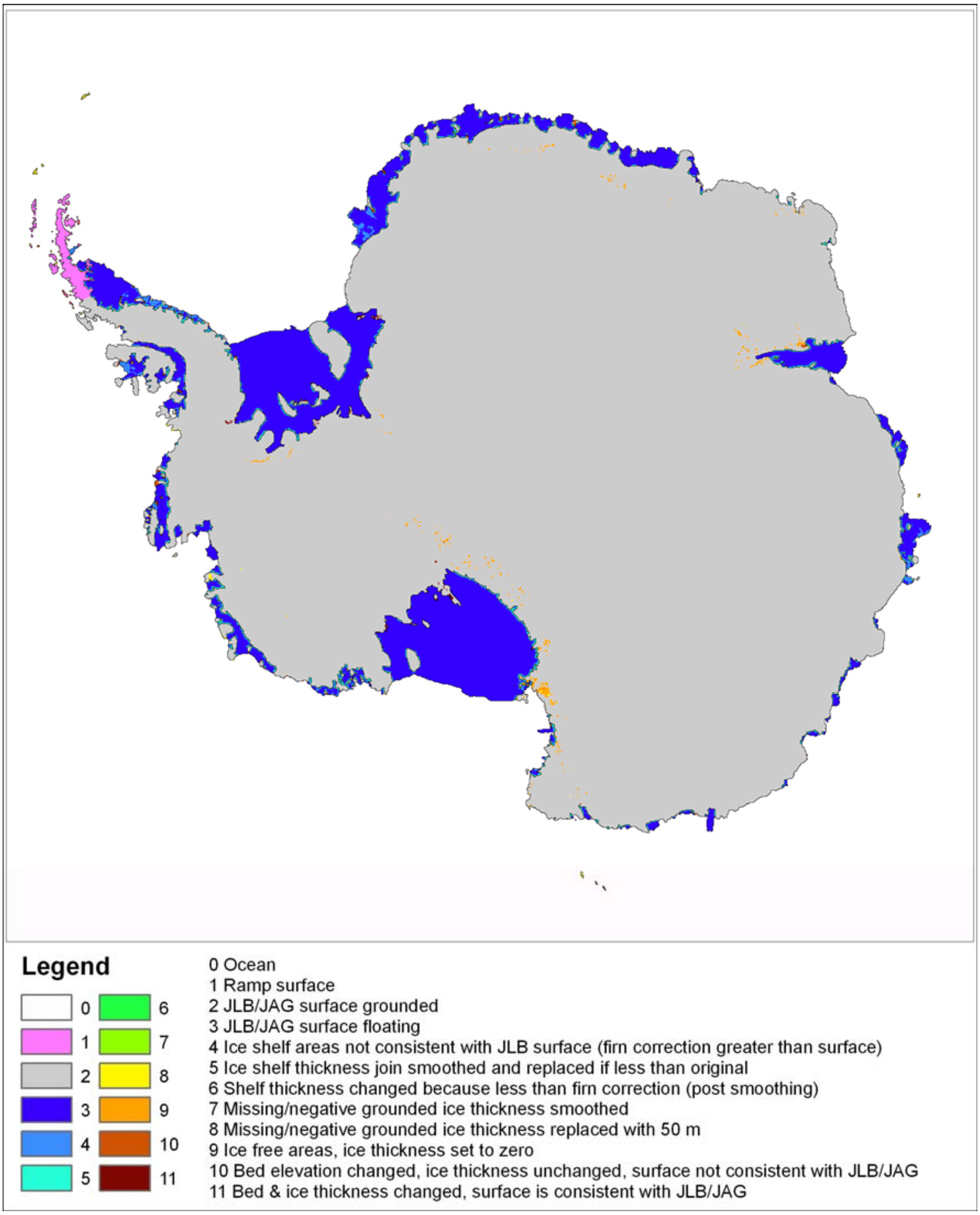


*Figure 13. Description of umask*

*Table 4. Summary of bmask values*

| Value | Description |
|---|---|
| 0 | BEDMAP |
| 1 | Areas > -300 m - reinterpolated (kriging) |
| 2 | Area next to Transantarctic Mountains - reinterpolated (spline) |
| 3 | Amundsen Sea small ice shelves reinterpolated (spline, with max depth derived from bathymetry) |
| 4 | PIG AGASEA/BBAS |
| 5 | Nitsche |
| 6 | Amery Ice Shelf kriging |
| 7 | Smoothed join |
| 8 | Excavated bed - original bathymetry minus depth to make it float minus extra depth (20 m) |
| 9 | AGASEA/BBAS bed |
| 10 | BEDMAP/AGASEA join |
| 11 | Combined surface minus combined ice thickness |
| 12 | Bed elevation changed, ice thickness unchanged, surface not consistent with JLB/JAG |
| 13 | Bed & ice thickness changed, surface is consistent with JLB/JAG |
| 14 | Ocean > -10 set to -10 |
| 15 | Excavated bed - original bathymetry minus depth to make it float minus extra depth (1 m) |

*Table 5. Summary of umask values*

| Value | Description |
|---|---|
| 0 | Ocean |
| 1 | Ramp surface |
| 2 | JLB/JAG surface grounded |
| 3 | JLB/JAG surface floating |
| 4 | Ice shelf areas not consistent with JLB/JAG surface (firn correction greater than surface) |
| 5 | Ice shelf thickness join smoothed and replaced if less than original |
| 6 | Shelf thickness changed because resulting surface  less than firn correction (post smoothing) |
| 7 | Missing/negative grounded ice thickness smoothed |
| 8 | Missing/negative grounded ice thickness replaced with 50 m |
| 9 | Ice free areas, ice thickness set to zero |
| 10 | Bed elevation changed, ice thickness unchanged, surface not consistent with JLB/JAG |
| 11 | Bed & ice thickness changed, surface is consistent with JLB/JAG |

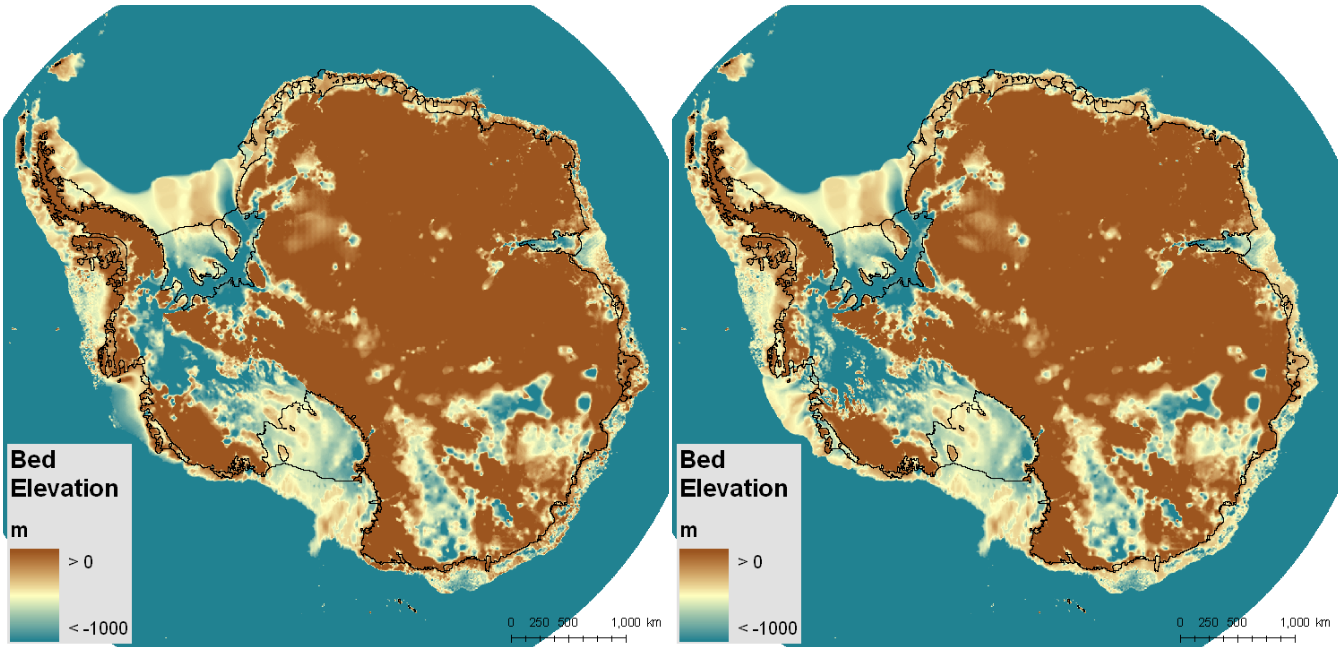


*a)* *b)*

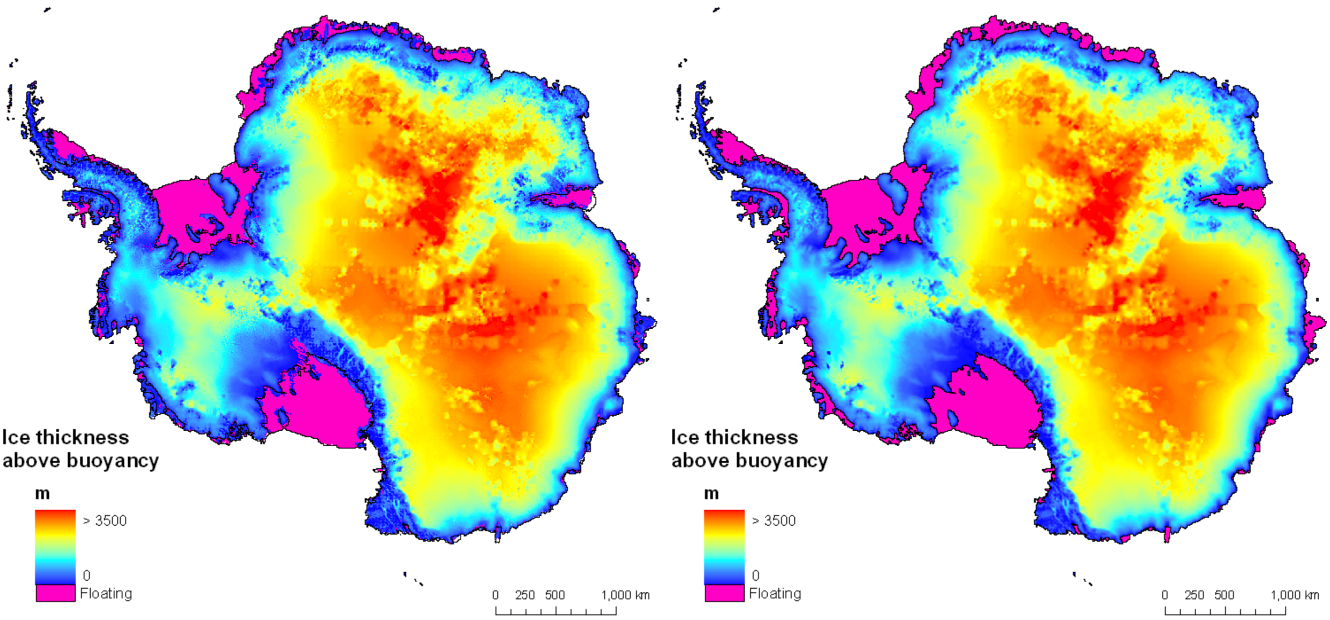


*c)* *d)*

*Figure 14. a) original BEDMAP, b) new dataset, c) ice thickness above buoyancy for BEDMAP, d) ice thickness above buoyancy for new dataset.*

### *4. Surface temperature*

The surface temperature dataset is described in Comiso (2000). The surface temperature estimates are derived from AVHRR infrared data. Annual mean temperatures from 1982-2004 were averaged to provide the surface temperature field (Fig. 15). The AVHRR data are currently available on a monthly basis at a resolution of 6.25 km from November 1978 to mid-2009 as part of an ongoing project (contact Joey Comiso).

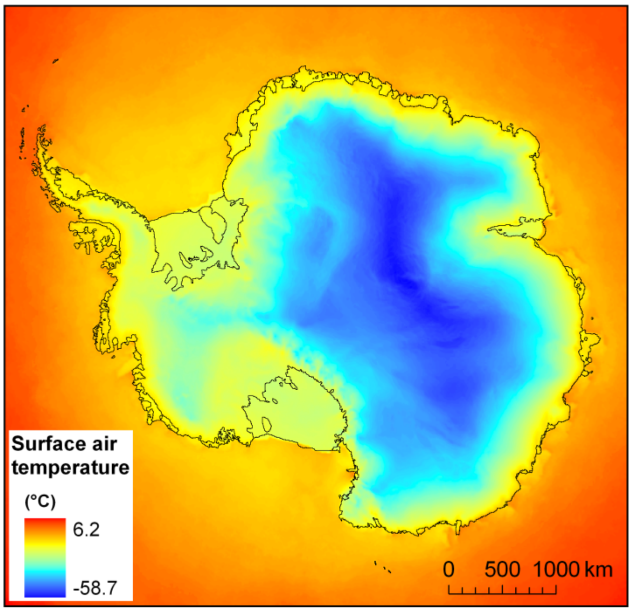


*Figure 15. Surface Temperature*

### *5. Accumulation*

#### *5.1 Athern et al. (2006)*

The accumulation dataset of Athern et al. (2006) was derived from interpolation of in situ point measurements, i.e. snow pits, ice cores and stake measurements. Passive microwave satellite data (firn emissivity) were used as a 'forcing field' to control the interpolation. The original data can be downloaded from: http://www.antarctica.ac.uk/bas_research/data/online_resources/snow_accumulation/. The data are supplied at a resolution of 25 km. The data were, here, interpolated onto the 5 km grid using spline interpolation. In the original dataset there is no data beyond the ice sheet, however, it would be useful to have values beyond the present day ice sheet. Hence, the accumulation data was extrapolated beyond the present day ice sheet, though these values have no physical basis, and are purely result of extrapolation from the ice covered values, and the interpolation method used, so should be used with caution. The accumulation dataset was masked using the -2000 m bathymetry contour (to provide data beyond the present day ice sheet, but to limit it to the continental shelf) (Fig. 16a).

#### *5.2 Van de Berg et al. (2006)*

The accumulation dataset of Van de Berg et al. (2006) is an output from the RACMO regional model (Van de Berg et al., 2006). The accumulation is generally higher than that of Vaughan (1999) and Athern et al., (2006), especially in data-sparse areas. The integrated accumulation exceeds previous estimates by up to 15 %. The data were provided as lat-lon point measurements, these were reprojected onto the polar stereographic grid and interpolated onto the 5 km grid using spline interpolation. The dataset was masked using the -2000 m bathymetry contour in the same way as the Athern et al. (2006) bathymetry (Fig. 16b), again, areas beyond the present day ice sheet are a result of the extrapolation process and the interpolation method used.

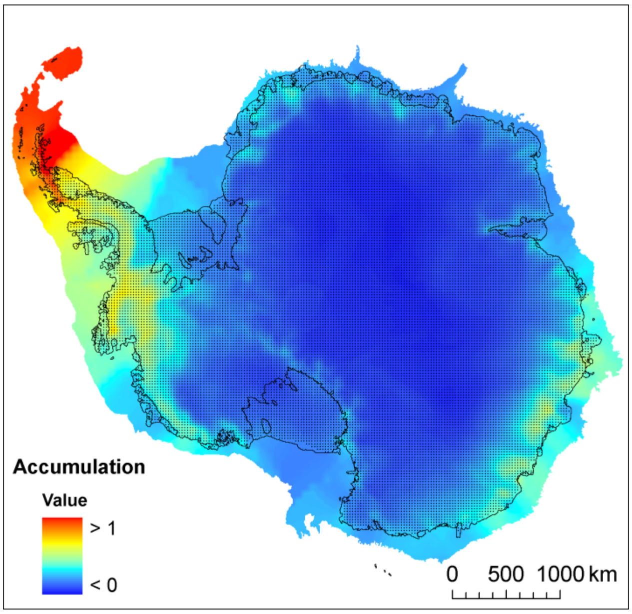


*a)*

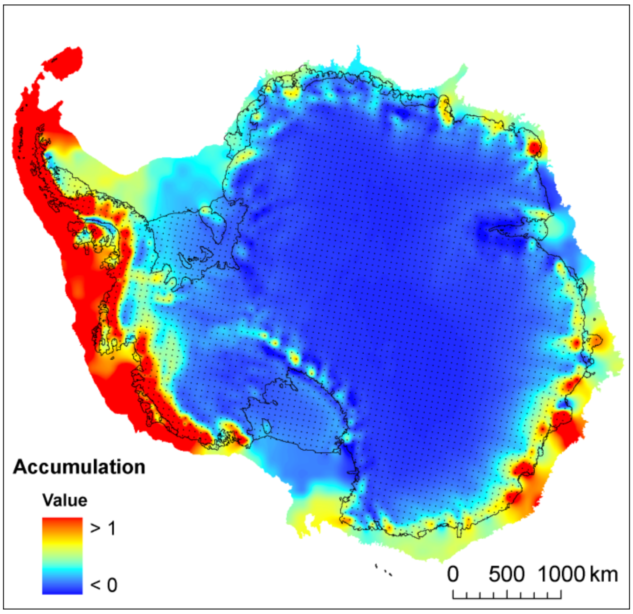


*b)*

*Figure 16. Accumulation datasets; a) Athern et al. (2006) accumulation, b) Van de Berg et al. (2006). (Black line is outline of mask, points indicate original data points).*

***6. Geothermal heat flux***

Two geothermal heat fluxes maps are provided in this dataset, which differ greatly from each other. The method of derivation is briefly described here and also the method of gridding the data. Note that the heat flux values are positive, some ice sheet models (including Glimmer-CISM), require these values to be negative.

***6.1 Shapiro & Ritzwoller (2004)***

Shapiro and Fitzwoller (2004) use a global seismic model of the crust and upper mantle to extrapolate existing heat flux measurements to areas where there is little data, using a 'structural similarity function'. The data were provided in lat-lons, but are also based on a geographic grid (see Fig. 17a). When converted to a polar stereographic projection, this creates problems in gridding straight to 5km resolution, due to the directionality of the points used in the interpolation procedure (see Fig. 17b). The gridding introduces elongated features which are not present in the original data.

The effective resolution of the data (in latitude anyway) is ~100 km. Therefore the data were first gridded on to a 100 km grid using spline interpolation (Fig. 17c). The 100 km grid points were then reinterpolated, again using spline interpolation, on to the 5 km grid (Fig. 17d). This reduces the elongated features whilst retaining most of the detail in the original dataset.

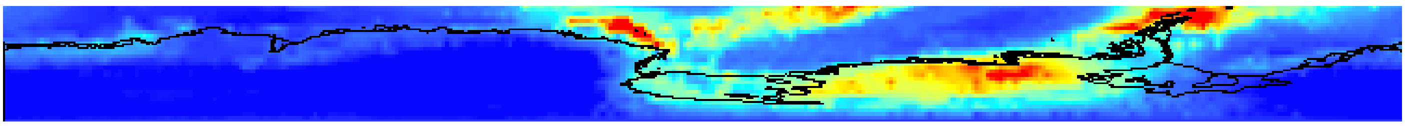

*a)*

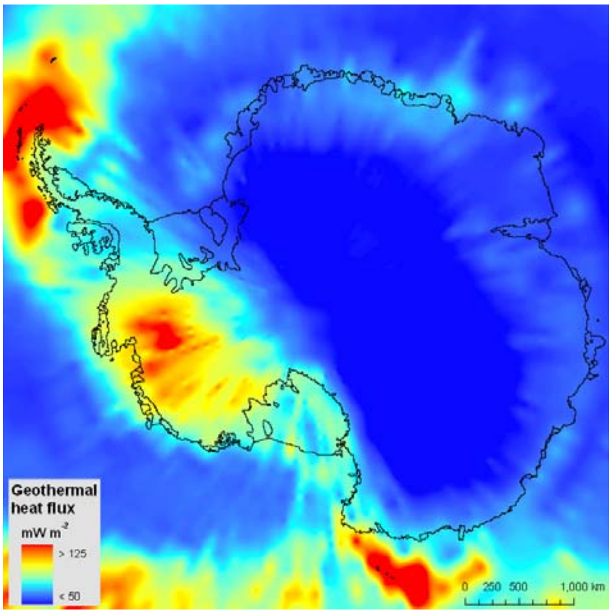


*b)*

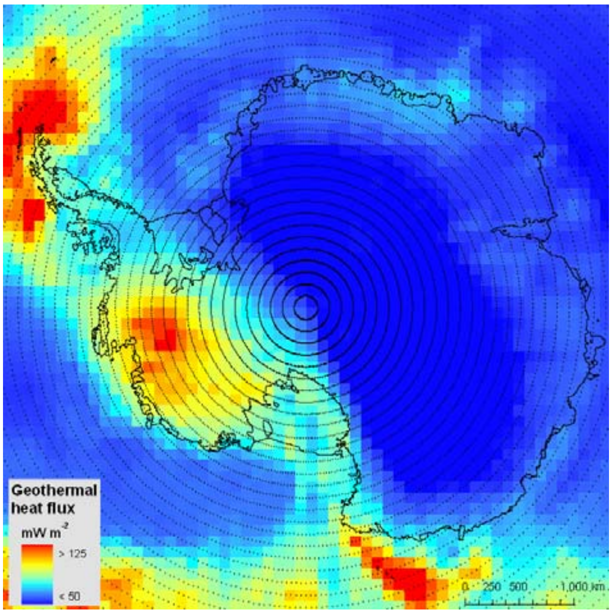


*c)*

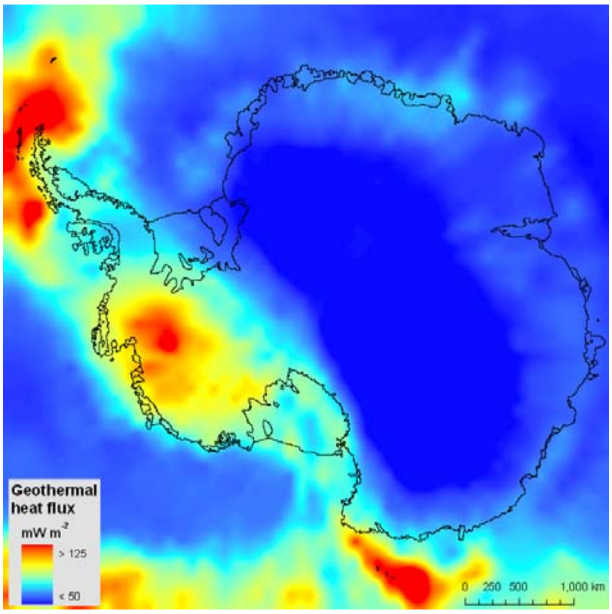


*d)*

*Figure 17. Geothermal heat flux from Shapiro and Ritzwoller (2004), a) original projection (lat-log), b) spline interpolation (5 km) on projected points (see c) for points), c) spline interpolation on to 100 km grid, the points indicate the original data points, d) 100 km data reinterpolated on to the 5 km grid.*

### *6.2 Fox Maule et al. (2005)*

The geothermal heat flux dataset of Fox Maule et al. (2005) was derived from satellite magnetic data and a thermal model. The point data provided were interpolated on to the 5 km grid using spline interpolation. The dataset was then masked using the -2000 m bathymetry contour buffer described in Section 5, as the points are limited to the grounded ice regions of Antarctica (Fig. 18).

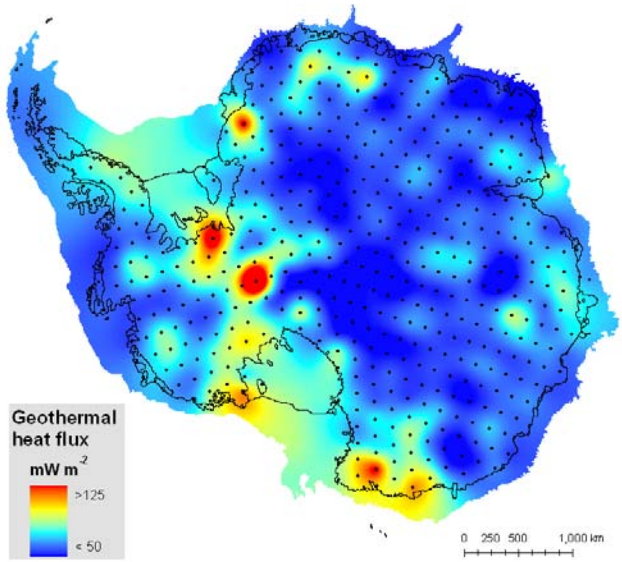


*Figure 18. Geothermal heat flux from Maule et al. (2005), the points indicate the original data points.*

### *7. Summary*

This document has detailed the steps taken in order to create a dataset suitable for high resolution numerical ice sheet modelling. It is hoped that the dataset will be useful to the community, but also that the importance of consistency within the ice sheet configuration datasets is demonstrated. The importance of a consistent ice sheet surface across the grounding line cannot be made strongly enough, as with the importance of a correct grounding line location. If a model is to accurately predict the future evolution of the ice sheet/ice streams it is important that the response is not just the model responding to inaccuracies in the input data. Whilst these will never be eradicated, it is important that they are minimised as far as possible.

### *Acknowledgements*

Funding for this project was provided by a UK Natural Environment Research Council (NERC) grant NE/E006108/1, The work was also greatly helped by collaboration within the framework of the EU Framework 7 project ice2sea.

### *Affiliations*

1. Department of Geography, Durham University, Durham, UK.
2. School of Geography, University of Exeter, Exeter, UK (Anne Le Brocq here from March 2010).
3. Bristol Glaciology Centre, Bristol University, Bristol, UK.
4. British Antarctic Survey, Cambridge, UK.
5. NASA Goddard Space Flight Center, Maryland, USA.
6. School of Ocean Sciences, Bangor University, Anglesey, UK.
7. Danish Climate Center, Danish Meteorological Institute, Copenhagen, Denmark.
8. Lamont-Doherty Earth Observatory of Columbia University, New York, USA.
9. Département de Sismologie, Institut de Physique du Globe de Paris, Paris, France.
10. Utrecht University, Utrecht, Netherlands.

### *References*

Arthern, R. J., Winebrenner, D. P., and Vaughan, D. G. (2006). Antarctic snow accumulation mapped using polarization of 4.3-cm wavelength microwave emission. Journal of Geophysical Research-Atmospheres 111, D06107, doi:10.1029/2004JD005667

Bamber, J.L., Gomez-Dans, J.L. and Griggs, J.A., (2009) A new 1 km digital elevation model of the Antarctic derived from combined satellite radar and laser data – Part 1: Data and methods, The Cryosphere, 3, 101-111.

Comiso, JC. (2000) Variability and trends in Antarctic surface temperatures from in situ and satellite infrared measurements, Jounal of Climate, 13 (10), 1674-1696.

Edwards, L.A. (2008), Unpublished PhD thesis, University of Bristol.

Fox Maule, C., Purucker, M., Olsen N., and Mosegaard K., (2005), Heat flux anomalies in Antarctica revealed by satellite magnetic data, Science, 309, 464–467.

Griggs, J. A. and Bamber, J. L., (2009a) A new 1 km digital elevation model of the Antarctic derived from combined satellite radar and laser data – Part 2: Validation and error estimates, The Cryosphere, 3, 113-123.

Griggs, J. A. and Bamber, J. L., (2009b) Ice shelf thickness over Larsen C, Antarctica, derived from satellite altimetry. Geophysical Research Letters, 36: Art. No. L19501. doi:10.1029/2009GL039527

Haran, T., Bohlander, J., Scambos, T.A., Painter, T. and Fahnestock, M. compilers. (2005, updated 2006) MODIS mosaic of Antarctica (MOA) image map. Boulder, Colorado USA: National Snow and Ice Data Center. Digital media.

Holt, J. W., Blankenship, D. D., Morse, D. L., Young, D. A., Peters, M. E., Kempf, S. D., Richter, T. G., Vaughan, D. G. and Corr, H. F. J., (2006), New boundary conditions for the West Antarctic Ice Sheet: Subglacial topography of the Thwaites and Smith glacier catchments, Geophysical Research Letters, 33, L09502, doi:10.1029/2005GL025561.

Le Brocq, A. M., Hubbard, A., Bentley, M. J., and Bamber, J. L. (2008). Subglacial topography inferred from ice surface terrain analysis reveals a large un-surveyed basin below sea level in East Antarctica. Geophysical research Letters. 34, L16503, doi: 10.1029/2008GL034728.

Liu, H., Jezek, K. and Li, B., (1999), Development of an Antarctic digital elevation model by integrating cartographic and remotely sensed data: A geographic information system based approach, Journal of Geophysical Research, 104(B10), 23,199–23,213

Lythe, M. B., Vaughan, D. G. and the BEDMAP Consortium (2001), BEDMAP: A new ice thickness and subglacial topographic model of Antarctica, Journal of Geophysical Research-Solid Earth, 106(B6), 11,335–11,351.

Nitsche, F.O., Jacobs, S., Larter, R.D. and Gohl, K., (2007) Bathymetry of the Amundsen Sea Continental Shelf: Implications for Geology, Oceanography, and Glaciology. Geochemistry, Geophysics, Geosystems,8: Q10009, doi:10.1029/2007GC001694.

Rutt, I.C., Hagdorn, M., Hulton, N.R.J. and Payne, A.J., (2009) The 'Glimmer' community ice sheet model. Journal of Geophysical Research., 114 (F2), F02004. (10.1029/2008JF001015.)

Scambos, T.A., Haran, T.M., Fahnestock, M.A., Painter, T.H. and Bohlander, J. (2007) MODIS-based Mosaic of Antarctica (MOA) data sets: Continent-wide surface morphology and snow grain size. Remote Sensing of Environment 111 (2-3), 242-257.

Shapiro, N.M. and Ritzwoller, M.H. (2004), Inferring surface heat flux distributions guided by a global seismic model: particular application to Antarctica, Earth and Planetary Science Letters, 223, 213-224.

Van de Berg, W. J., van den Broeke, M. R. and van Meijgaard, E., (2006) Reassessment of the Antarctic surface mass balance using calibrated output of a regional atmospheric climate model, Journal of Geophysical Research 111, D11104, doi:10.1029/2005JD006495.

Van den Broeke, M. R., van de Berg, W. J. and van Meijgaard, E., (2008) Firn depth correction along the Antarctic grounding line, Antarctic Science, doi: 10.1017/S095410200800148X.

Vaughan, D. G., Bamber, J. L., Giovinetto, M., Russell, J. and Cooper, A. P. R., (1999) Reassessment of net surface mass balance in Antarctica, Journal of Climate, 12(4), 933–946

Vaughan, D. G., Corr, H. F. J., Ferraccioli, F., Frearson, N., O'Hare, A., Mach, D., Holt, J., Blankenship, D., Morse, D. and Young, D. A. (2006), New boundary conditions for the West Antarctic ice sheet: subglacial topography beneath Pine Island Glacier, Geophysical Research Letters, 33, L09501, doi:10.1029/2005GL025588.